

Optically encoded microspheres for high-throughput analysis of genes and proteins

Xiaohu Gao^a, Minyong Han^b, and Shuming Nie^{a,c}

^aWallace Coulter Department of Biomedical Engineering, Georgia Institute of Technology and Emory University, 1639 Pierce Drive, Suite 2001, Atlanta, GA 30322.

^bInstitute of Materials Research and Engineering (IMRE), 3 Research Link, Singapore 117602; Department of Materials Science, National University of Singapore, 10 Kent Ridge Crescent, Singapore 119260.

^cDepartments of Chemistry, Hematology and Oncology, and the Winship Cancer Institute, Emory University School of Medicine, 1365 Clifton Road, Suite B4100, Atlanta, GA 30322. Correspondence: Shuming Nie; email: snie@emory.edu.

ABSTRACT

We have developed a novel optical coding technology for massively parallel and high-throughput analysis of biological molecules. Its unprecedented multiplexing capability is based on the unique optical properties of semiconductor quantum dots (QDs) and the ability to incorporate multicolor QDs into small polymer beads at precisely controlled ratios. The use of 10 intensity levels and 6 colors could theoretically code one million nucleic acid or protein sequences. Imaging and spectroscopic studies indicate that the QD tagged beads are highly uniform and reproducible, yielding bead identification accuracies as high as 99.99% under favorable conditions. DNA hybridization results demonstrate that the coding and target signals can be simultaneously read at the single-bead level. This spectral coding technology is expected to open new opportunities in gene expression studies, high-throughput screening, and medical diagnosis.

Keywords: quantum dots, nanocrystals, high-throughput, multiplexing, genomics, proteomics, biomedical diagnostics, drug screening, spectral barcoding

1. INTRODUCTION

Cells are complicated with a great deal of intricate molecular events occurring at the same time. Errors within cellular genetic makeup and protein networks may lead to life-threatening diseases, such as malignancy. Therefore the demand of technologies that can analyze these biomolecules rapidly and simultaneously represents a crucial challenge for large-scale genomic and proteomic research. Currently several powerful techniques have been developed for such analysis, including planar DNA microchips^{1,2} and dye-encoded microspheres³. These technologies have yielded a large amount of genetic and cellular information. Biochips are well suited for large-scale analysis, while the encoded bead technology offers more flexibility in target selection. Most recently, a NanobarcodeTM technology, which enables the measurements of many thousands of analytes in parallel, has been reported by Natan and coworkers based on differential reflectivity of submicrometer metallic stripes⁴. However, the reliability of its readout mechanism is unclear, and conjugation of biomolecules to metallic stripes has not been fully investigated.

To address some of these problems, we have developed a novel spectral coding technology for high throughput analysis of genes and proteins. This technology is based on the unique optical properties of QDs^{5,6} and the ability to incorporate multicolor QDs into small polymer beads in a precisely controlled manner⁷. The basic concept is that micrometer-sized polymer beads could not only have molecular recognition abilities, but also build-in codes for rapid target identification. For example, biomolecular probes can be conjugated to the bead surface, while a unique optical code is embedded in the bead's interior. In comparison with organic dyes, luminescent QDs are better fluorophores for this application

because they have narrow and symmetrical emission spectra, broad excitation profiles, and improved photostability. These properties enable the simultaneous excitation of multicolor QDs with a single light source (single wavelength).

A key feature of spectral coding is wavelength and intensity multiplexing. The use of 10 intensity levels (0~9) at a single color provides 9 codes (note that level 0 cannot be differentiated from the background level). The number of color and intensity combinations increases rapidly when multiple colors and intensities are used at the same time. For example, a 3-color/10-intensity coding scheme will yield 999 codes. It should be noted that 1:0:0, 0:1:0 and 0:0:1 are three unique codes although 0:0:0 is not a useful one. Table 1 shows the theoretical calculations of the total combination number using m colors and n intensity levels. If 6 colors and 10 intensity levels are employed, the coding capacity can reach ca. one million.

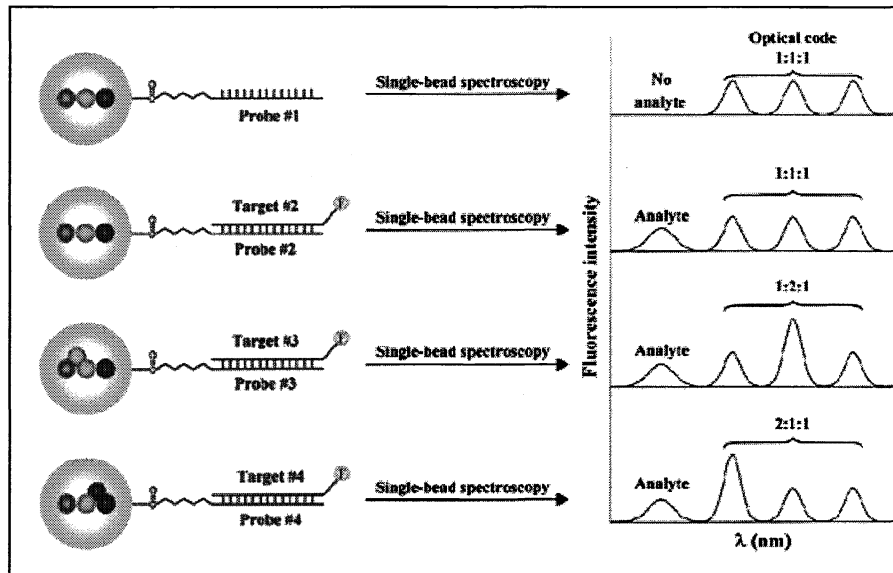


Figure 1. Schematic illustration of DNA hybridization assays using QD-tagged beads. Probe oligos (No. 1–4) were conjugated to the beads by cross-linking, and target oligos (No. 1–4) were detected with a blue fluorescent dye, Cascade Blue. After hybridization, nonspecific molecules and excess reagents were removed by washing. The coding signals identify the DNA sequence, whereas the target signal indicates the presence and abundance of that sequence.

To demonstrate the use of QD-tagged beads for biological assays, we designed a model DNA hybridization system using oligonucleotide probes and triple-color encoded microbeads. As shown in Figure 1, oligonucleotide probes are covalently conjugated to the bead surface, while target DNA molecules are labeled with a fluorescent dye via a biotin-streptavidin linker. When the beads and an unknown target sample are mixed, hybridization takes place when the probe sequence is complementary to the target sequence. The coding and the target signals can be detected by optical spectroscopy at the single-bead level. The coding signals identify the DNA sequence, whereas the target signal indicates the presence and the abundance of that sequence.

Based on these multiplexed DNA hybridization studies, we envision the use of this “beadcoding” approach in practical genomic and proteomic research with integration of microfluidic devices and construction of a library of encoded beads and probe molecules.

Table 1 Theoretical coding numbers of QD-tagged polymeric beads using m colors of QDs and n intensity level of each.

Wavelengths	Intensity Levels	Combination No.	Useful IDs
1	10 (0 ~ 9)	10^1	10^1-1
2	10 (0 ~ 9)	10^2	10^2-1
3	10 (0 ~ 9)	10^3	10^3-1
.	.	.	.
6	10 (0 ~ 9)	10^6	10^6-1
8	10 (0 ~ 9)	10^8	10^8-1
m	n (0 ~ n-1)	n^m	n^m-1

2. EXPERIMENTAL

2.1. Materials and equipment. Technical grade (90%) trioctylphosphine oxide (TOPO), trioctylphosphine (TOP, 99% pure), hexamethyldisilathiane ((TMS)₂S), acrylic acid (99%), polyvinylpyrrolidone, and a polymerization initiator (AIBN, 98%) were purchased from Aldrich and were used without further purification. Dimethylcadmium (CdMe₂) and dimethylzinc (ZnMe₂, 10% wt in hexane) were obtained from Alfa and Strem, respectively. CdMe₂ was filtered through a 0.2 μm filter in an inert atmosphere box. Styrene (99%) and divinylbenzene (80%) were purchased from Fluka. Biotinylated oligo probes (26-mer oligonucleotides, HPLC-purified) were purchased from TriLink Biotechnology (San Diego, CA). The probe and target sequences are listed in Table 2.

2.2. Preparation of highly luminescent CdSe/ZnS QDs. CdSe stock solution was prepared by dissolving 100 mg Se shot and 120 μl Cd(Me)₂ in TOP. ZnS stock solution was prepared by dissolving 5 ml of 10% (w/w) Zn(Me)₂ in hexane and 1 ml (TMS)₂S in TOP. In a typical synthesis, 12.5 g TOPO was heated to 200 °C and refluxed for 20 min to remove trace oxygen. Then the temperature was briefly raised to 360 °C. The CdSe stock solution was quickly injected into the hot TOPO solution using a large-bore needle. The reaction was either stopped immediately by removing the heating or allowed to continue after lowering the temperature to 300 °C. The nanocrystal size was monitored by UV-vis measurement of reaction solution aliquots. The reaction was stopped by lowering the temperature to 100 °C after the desired size was achieved. The total heating process lasted from minutes to hours. The ZnS stock solution was added at this point, and the reaction was stirred overnight. The reaction mixture was cooled to room temperature and excess TOPO was removed by methanol precipitation.

Table 2. Probe and target oligonucleotide sequences. Each sequence is biotinylated via a poly T spacer.

Probes or targets	Sequences
Probe 1	5' Biotin-(T) ₅ -TCA AGG CTC AGT TCG AAT GCA CCA TA 3'
Target 1	5' Biotin-(T) ₅ -TAT GGT GCA TTC GAA CTG AGC CTT GA 3'
Probe 2	5' Biotin-(T) ₅ -CCG TAC AAG CAT GGA ACG GCT TTT AC 3'
Target 2	5' Biotin-(T) ₅ -GTA AAA GCC GTT CCA TGC TTG TAC GG 3'
Probe 3	5' Biotin-(T) ₅ -TAC TCA GTA GCG ACA CAT GGT TCG AC 3'
Target 3	5' Biotin-(T) ₅ -GTC GAA CCA TGT GTC GCT ACT GAG TA 3'
Probe 4	5' Biotin-(T) ₅ -ACT AAG AGT TGA CAG GGA CCT TGT CT 3'
Target 4	5' Biotin-(T) ₅ -AGA CAA GGT CCC TGT CAA CTC TTA GT 3'

2.3. Preparation of multicolor QD-tagged microbeads. Beads were synthesized by emulsion polymerization of styrene (98% vol/vol), divinylbenzene (1% vol/vol), and acrylic acid (1% vol/vol) at 70°C^{8, 9}. The reaction was initiated by AIBN and allowed to polymerize for 10 hours. Transmission electron microscopy revealed that the beads had a 1.2-μm diameter with a standard deviation of 2–3% in

diameter. Incorporation of QDs was achieved by swelling the beads in a solvent mixture containing 5% chloroform and 95% (vol/vol) propanol or butanol, and by adding a controlled amount of ZnS-capped CdSe QDs to the mixture. The embedding process was complete within 30 minutes at room temperature. Before DNA conjugation, the encoded beads were protected by using 3-mercaptopropyl trimethoxysilane, which polymerized inside the pores upon addition of a trace amount of water.

2.4. DNA hybridization assay and single bead spectroscopy. Standard protocols were used to covalently attach streptavidin molecules to the carboxylic acid groups on the bead surface¹⁰. In brief, the QD encoded beads were incubated in 5 mg/ml EDAC for 30 minutes to activate carboxylic groups on the bead surface. Streptavidin (10mg/ml) was conjugated to the beads via the creation of an amide bond. Nonspecific binding sites were blocked by using BSA (0.5 mg/ml) in PBS buffer (pH 7.4). 5' Biotinylated oligo probes were linked to the beads via the attached streptavidin, and the target oligos were labeled with avidin–Cascade Blue conjugate. DNA hybridization was performed in 0.1% sodium dodecyl sulfate PBS buffer at 40°C for 30 min. Before fluorescence measurements, the beads were purified by two rounds of centrifugation. Single-bead spectroscopy was accomplished using a fluorescence microscope equipped with a single-stage spectrograph and a CCD detector. Near-UV excitation (330–385 nm) was provided by a 100 W mercury lamp.

3. RESULTS AND DISCUSSION

3.1. Optical properties of QDs. Recent development in organometallic synthesis has produced a new class of fluorophore, quantum dots. These nanometer-sized semiconductor crystals provide novel optical properties that are not available with traditional organic dyes. Particularly, the emission wavelength can be continuously and precisely tuned by varying the particle size. QDs also have broad absorption spectra, which enables simultaneous excitation of multicolor dots. Figure 2 shows a fluorescent image of 10 distinguishable colors of CdSe/ZnS dots excited with a UV lamp, and Figure 3 shows the corresponding emission spectra. As noted earlier, this kind of simultaneous excitation is not possible with organic dyes. In addition, a thin layer of ZnS coating on CdSe dots significantly increases the quantum yield and photostability. These unique optical properties make QDs ideal fluorophores for ultrasensitive and multiplexing biological assays.

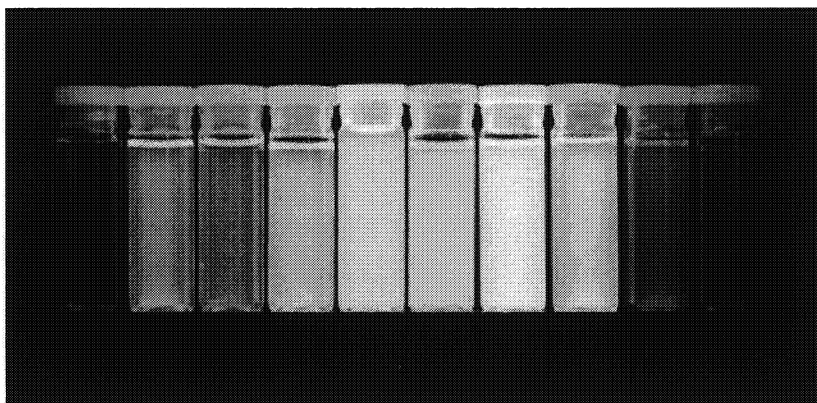


Figure. 2. True color fluorescent image of a series of ZnS-capped CdSe QDs, simultaneously excited with a handheld UV lamp. The colors are clearly distinguishable one from another.

3.2. Spectral coding of microbeads. The potential of spectral coding has been recognized by other researchers¹¹⁻¹⁴. However, previous studies were based on organic dyes or lanthanide compounds. The multiplexing level was limited by the number of spectrally resolvable fluorophores. Therefore, luminescent QDs are superior substitutes of dyes for this purpose due to their unique optical properties. A key issue is how to incorporate multicolor QDs into micrometer-sized beads in a precisely controlled manner. We

solved this problem by synthesis of porous and monodispersed polymeric beads and formulation of the incorporation conditions. Polystyrene beads were synthesized by suspension co-polymerization of styrene, divinylbenzene, and acrylic acid. These beads have a hydrophobic interior and carboxylic acid groups on their surface. The pore size has been estimated to be 5-10 nm based on the size of QDs. We note that further experiments are needed for quantitative determination. Five color QDs were allowed to uniformly diffuse into the polymer beads, with their emission wavelength remaining roughly identical to those of the original QDs. Figure 4 shows a multicolor fluorescence image obtained from a mixture of these beads spread on a glass surface. The five emission colors are simultaneously excited and clearly distinguishable from one another.

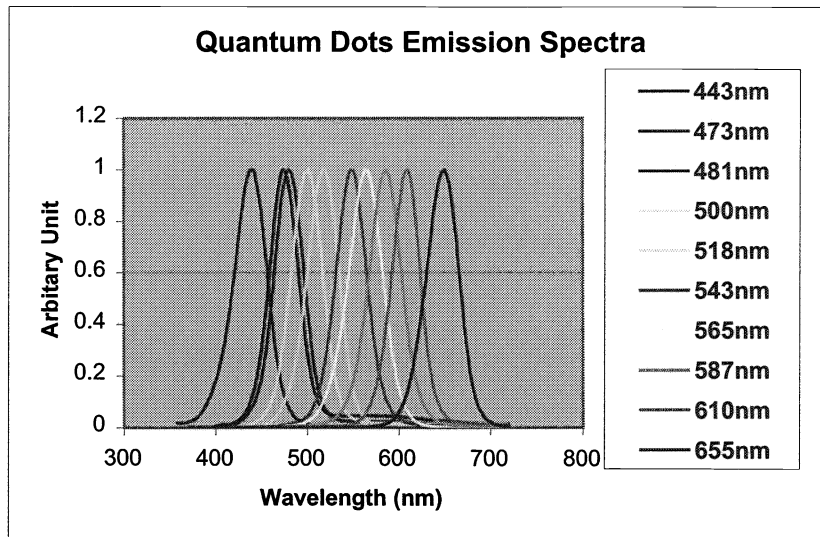


Figure 3. Size-dependent fluorescence spectra corresponding to the samples shown in Figure 2.

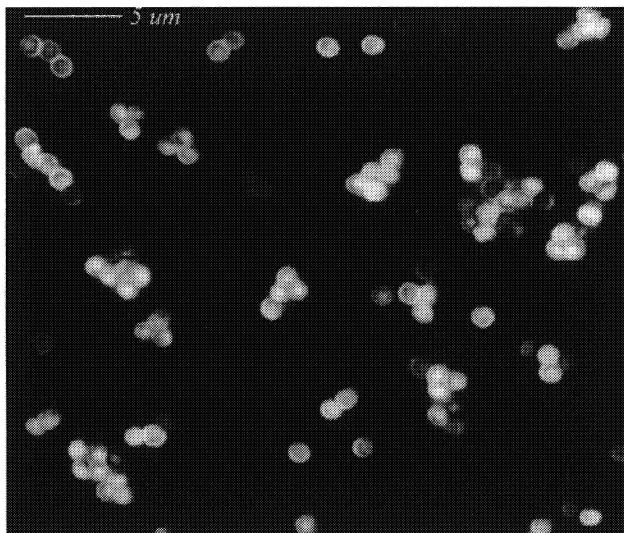


Figure 4. True color image of a mixture of CdSe/ZnS QD-tagged beads emitting single-color signals at 484, 508, 547, 575, and 611 nm. The beads were spread and immobilized on a polylysine-coated glass slide, which caused a slight clustering effect.

A key question was whether the embedded QDs would aggregate inside of the beads, which could cause spectral line-width broadening, peak shifting and energy transfer. To our surprise, the fluorescence spectra

of QD-tagged beads were narrower by $\sim 10\%$ than those of original QDs in solution, and the emission maxima remain unchanged. We believe that the bead's porous structure acts as a matrix to spatially separate the embedded QDs, as well as a filter to block the incorporation of large particles and aggregates in a heterogeneous population. Confocal imaging studies indicate that the QDs are mainly located in the outer 25% of the bead's radius, similar to the spatial distribution of organic dyes in polystyrene beads¹⁵. Our calculation indicates that the average separation distance is much larger than the Förster energy transfer radius for QDs^{16, 17}. The uniformity and reproducibility of these QDs encoded beads were further analyzed with a single bead spectrometer. Figure 5 shows 10 histogram plots, each corresponding to one of the 10 intensity levels. Statistical analysis shows that the relative standard deviations are in the range of 5 to 15 % (depending on the intensity levels). A major source of the errors appears to be the intrinsic variation in bead size (2-3% in diameter). Even in the presence of these errors, the histograms reveal that there is no intensity overlap among the first six levels at four standard deviations ($\pm 4\sigma$), and no overlap at three standard deviations ($\pm 3\sigma$) for the last four levels. Thus, we estimate that the bead identification accuracies are as high as 99.99% under favorable conditions.

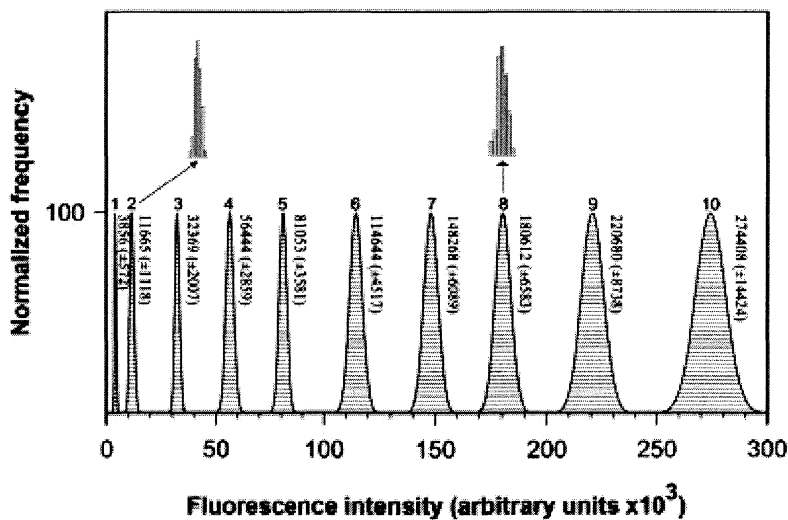


Figure 5. Spectroscopic analysis of single-bead fluorescence intensities. Each histogram plots is corresponding to one of the ten intensity levels, derived from 100-200 measurements. On the right side of each curve is shown the average fluorescence intensity as well as the standard deviation (in parentheses). Representative raw data are shown for levels 2 and 8.

Following the single-color studies, experiments on multicolor QD coded beads were carried out. In a typical 3-color coding scheme, the fluorescent intensity ratio of red, green and blue dots was pre-determined by a fluorometer. This ratio remained unchanged for low loading levels, which was validated by single bead spectroscopy. Figure 6 shows a *true color* image of the 3-color coded beads with 1:1:1 intensity ratio. The white fluorescence is due to the precise emission balance from the three primary colors. For high loading levels of QDs, we preferred to incorporate QDs in a sequential way, meaning that red QDs were added first, and then green and blue dots were embedded afterward. This is not only because red QDs have a bigger size and slower diffusion rate, but also the beads' small pore sizes are unfavorable for their incorporation.

To preserve the optical properties of the embedded QDs under a broad range of experimental conditions, the porous beads were shrunk with polar solvents and sealed with a thin layer of silica coating sequentially. 3-mercaptopropyltrimethoxysilane was polymerized inside the pores upon addition of trace amount of water.

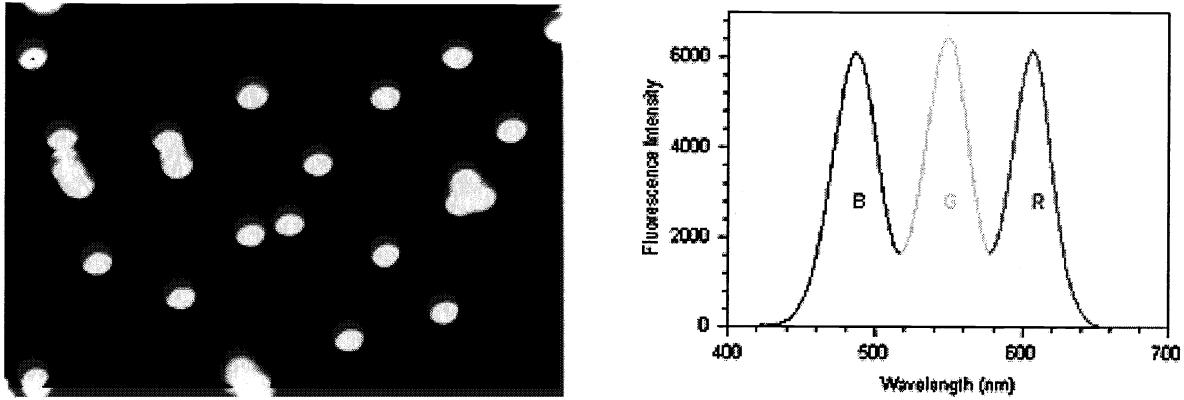


Figure 6. Triple color QD-tagged beads with precisely controlled fluorescence intensities. (Left) Fluorescence image of color-balanced beads. (Right) Single-bead fluorescence spectrum, showing three separated peaks (484, 547, and 608 nm) with nearly equal intensities.

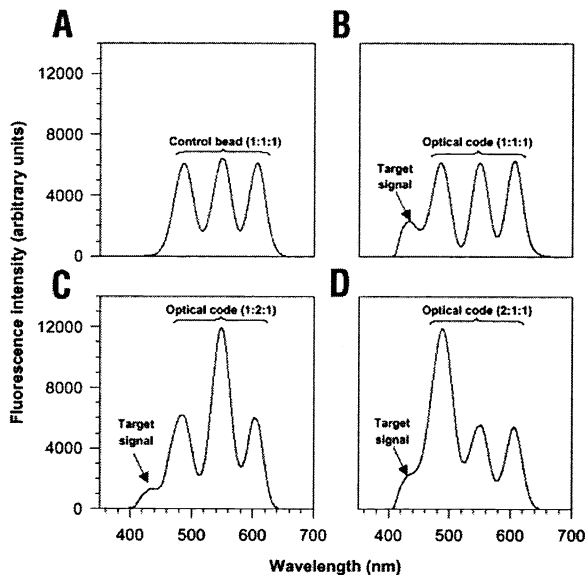


Figure 7. DNA hybridization assays using multicolor encoded beads. (A) Fluorescence signals obtained from a single bead with the code 1:1:1 (corresponding to Probe 1), after exposure to a control DNA sequence (Target 4). (B) Fluorescence signals of a single bead with the code 1:1:1, after hybridization with its target (Target 1). (C) Fluorescence signals of a single bead with the code 1:2:1 (Probe 2), after hybridization with its target (Target 2). (D) Fluorescence signals of a single bead with the code 2:1:1 (Probe 3), after hybridization with its target (Target 3).

3.3. Application in multiplexed bioassays. Figure 7 shows the assay results of one mismatched and three complementary oligonucleotides hybridized to the triple-color encoded beads. The code 1:1:1 corresponds to the oligo probe 1 (see Table 2). No analyte fluorescence was detected when noncomplementary sequences (target 4) were used for hybridization (A). This result showed a high degree of sequence specificity and a low level of nonspecific adsorption. Analyte fluorescence signals were observed only in the presence of complementary targets, as shown in Figure 7B–D.

The surface of internally color-coded polystyrene beads can be easily modified with other functional groups, such as amines and aldehydes¹⁰. This will provide variety options of biomolecules conjugation chemistry, which consequently enables many analytic schemes. Examples include DNA-DNA, avidin-biotin, receptor-ligand, enzyme-substrate, lectin-carbohydrate and protein A-immunoglobulin reactions.

4. CONCLUSION

We have developed a multiplexed spectral coding technology, based on the unique optical properties of semiconductor QDs and our ability to incorporate them into polymeric beads at precisely controlled ratios. Model DNA hybridization studies demonstrate that the coding and target signals can be simultaneously read at the single-bead level. We envision that this spectral coding technology will enable multiplexed, high-throughput profiling of genes and proteins, and will impact both basic biomedical research and clinical investigations.

5. REFERENCES:

1. S. A. Fodor, "DNA sequencing - massively parallel genomics", *Science* **277**, pp. 393, 1997.
2. A. P. Blanchard, and L. Hood, "Sequence to array: probing the genome's secrets", *Nat. Biotechnol.* **14**, pp.1649, 1996.
3. D. R. Walt, "Molecular biology - bead-based fiber-optic arrays", *Science* **287**, pp. 451-452, 2000.
4. S. R. Nicewarner-Pena, R. G. Freeman, B. D. Reiss, L. He, D. J. Pena, I. D. Walton, R. Cromer, C. D. Keating, and M. J. Natan, "Submicrometer metallic barcodes", *Science* **294**, pp. 137-141, 2001.
5. A. P. Alivisatos, "Semiconductor clusters, nanocrystals, and quantum dots", *Science* **271**, pp. 933-937, 1996.
6. M. Nirmal, and L. E. Brus, "Luminescence photophysics in semiconductor nanocrystals", *Acc. Chem. Res.* **32**, pp. 407-414, 1999.
7. M. Han, X. Gao, J. Z. Su, and S. Nie, "Quantum-dot-tagged microbeads for multiplexed optical coding of biomolecules", *Nat. Biotechnol.* **19**, pp. 631-635, 2000.
8. P. H. H. Hermkens, H. C. J. Ottenheijm, and D. Rees, "Solid-phase organic reactions: a review of the recent literature", *Tetrahedron* **52**, pp. 4527-4554, 1996.
9. B. Z. Yang, L. W. Chen, and W. Y. Chiu, "Effects of acrylic acid on number density of polymer particles in emulsifier-free emulsion copolymerization of styrene and acrylic acid", *Polymer J.* **29**, pp. 737-743, 1997.
10. G. T. Hermanson, *Bioconjugate techniques*, Academic Press, New York, 1996.
11. R. J. Fulton, R. L. McDade, P. L. Smith, L. J. Kienker, and J. R. Jr. Kettman, "Advanced multiplexed analysis with the FlowMetrix (TM) system", *Clin. Chem.* **43**, pp. 1749-1756, 1997.
12. F. J. Steemers, J. A. Ferguson, and D. R. Walt, "Screening unlabeled DNA targets with randomly ordered fiber-optic gene arrays", *Nat. Biotechnol.* **18**, pp. 91-94, 2000.
13. J. A. Ferguson, T. C. Boles, C. P. Adams, and D.R. Walt, "A fiber-optic DNA biosensor microarray for the analysis of gene expression" *Nat. Biotechnol.* **14**, pp. 1681-1684, 1996.
14. J. A. Ferguson, F. J. Steemers, and D. R. Walt, "High-density fiber-optic DNA random microsphere arrays", *Anal. Chem.* **72**, pp. 5618-5624, 2000.
15. Y. Z. Zhang, C. R. Kemper, and R. P. Haugland, "Microspheres with fluorescent spherical zones", US 5,786,219, 1998.
16. C. R. Kagan, C. B. Murray, M. Nirmal, and M. G. Bawendi, "Electronic energy transfer in CdSe quantum dot solids", *Phys. Rev. Lett.* **76**, pp. 1517-1520, 1996.
17. O. I. Micic, K. M. Jones, A. Cahill, and A. J. Nozik, Optical, electronic, and structural properties of uncoupled and close-packed arrays of InP quantum dots. *J. Phys. Chem. B* **102**, pp. 9791-9796, 1998.